Chemical Technology Division

ANL-95/12

Laboratory Testing of Glasses for Lockheed Idaho Technology Co. Fiscal Year 1994 Report

by A. J. G. Ellison, S. F. Wolf, and J. K. Bates

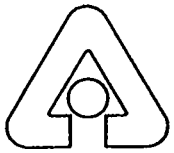

Argonne National Laboratory, Argonne, Illinois 60439
operated by The University of Chicago
for the United States Department of Energy under Contract W-31-109-Eng-38

Chemical Technology Division

Reproduced from the best available copy.

Available to DOE and DOE contractors from the
Office of Scientific and Technical Information
P.O. Box 62
Oak Ridge, TN 37831
Prices available from (615) 576-8401

Available to the public from the
National Technical Information Service
U.S. Department of Commerce
5285 Port Royal Road
Springfield, VA 22161

DISCLAIMER

Portions of this document may be illegible in electronic image products. Images are produced from the best available original document.

Distribution Category:
Nuclear Waste Management
(UC-510)

ANL-95/12

ARGONNE NATIONAL LABORATORY
9700 South Cass Avenue
Argonne, Illinois 60439

LABORATORY TESTING OF GLASSES FOR LOCKHEED IDAHO TECHNOLOGY CO. FISCAL YEAR 1994 REPORT

by

A. J. G. Ellison, S. F. Wolf, and J. K. Bates

Chemical Technology Division

April 1995

TABLE OF CONTENTS

LIST OF FIGURES

LIST OF TABLES

LABORATORY TESTING OF GLASSES FOR LOCKHEED IDAHO TECHNOLOGY CO. FISCAL YEAR 1994 REPORT

A. J. G. Ellison, S. F. Wolf, and J. K. Bates

ABSTRACT

Two vitreous materials supplied by Lockheed Idaho Technology Co. (LITCO), referred to as Formula 127 and Formula 532, have been subjected to accelerated durability tests to measure their long-term performance. Formula 127 consists of a glass matrix containing 5-10 vol % fluorite (CaF_2) as a primary crystalline phase. It shows low releases of glass components to solution in 7-, 28-, 70-, and 140-day Product Consistency Tests performed at 2000 m^{-1} at 90°C. In these tests, release rates for glass-forming components were similar to those found for durable waste glasses. The Ca and F released by the glass as it corrodes appear to reprecipitate as fluorite. Formula 532 consists of a glass matrix containing 5-10 vol % of an Al-Si-rich primary crystalline phase. The release rates for components other than aluminum are relatively low, but aluminum is released at a much higher rate than is typical for durable waste glasses. Secondary crystalline phases form relatively early during the corrosion of Formula 532 and appear to consist almost entirely of the Al-Si-rich primary phase (or a crystal with the same Al:Si ratio) and a sodium-bearing zeolite. Future test results are expected to highlight the relative importance of primary and secondary crystalline phases to the rate of corrosion of Formula 127 and Formula 532.

I. INTRODUCTION

The purpose of this project is to measure the intermediate and long-term durability of vitrified waste forms developed by Lockheed Idaho Technology Co. (LITCO) for the immobilization of calcined radioactive wastes at Idaho National Engineering Laboratory (INEL). Objectives of this work include the following:

- Provide LITCO with information that can be used in a performance assessment model to determine the source term of radioactive components in a geologic repository;
- Assist LITCO in optimizing waste form composition;
- Delineate the corrosion mechanisms of vitreous waste forms;
- Determine the approach to solution saturation as a glass reacts with water;
- Determine the identities and order of appearance of secondary crystalline phases formed after solution saturation.

The glasses tested in this program during FY 1994 are Formula 127 and Formula 532. This report summarizes experimental results obtained during FY 1994.

The objective of waste immobilization is to limit the release of radioactive elements to the environment during the period of controlled release. In a geologic repository, the most important avenue for release of radionuclides into the environment is reaction of a waste form with groundwater. When a waste form comes in contact with liquid water or water vapor, reactions occur that physically and chemically alter the waste form and result in dissolution of glass components into the aqueous phase. The initial rate of reaction, or forward rate, is highest when waste form corrosion products in solution are very dilute. As the reaction proceeds, the buildup of corrosion products in solution reduces the chemical potential gradient between waste form and water, and the rate of reaction slows. After prolonged contact with water, or as water evaporates from the surface of the waste form, the concentration of dissolved glass components will become high enough that secondary crystalline phases precipitate from solution. If the rate of growth of the secondary phases exceeds the rates of release of their components from the glass, the solution concentration of glass components will be maintained at the saturation value and the rate of glass corrosion will accelerate. Information about the forward rate, the intermediate corrosion rate and approach to saturation, and the corrosion rate after secondary phase formation are all required in a performance assessment to model glass behavior.

Information about these stages in the corrosion process is obtained by using accelerated laboratory tests. The two primary means of accelerating the rate of corrosion are increasing the temperature at which a test is performed and increasing the ratio of sample surface area to solution volume (SA/V). When SA/V is low (e.g., 10 m^{-1}), dissolved glass components remain dilute in solution for an extended period of time; thus, low SA/V tests are used to determine the forward rate of waste form reactions. They can also be used to distinguish between the rates of initial reaction of a glass and of primary crystalline phases contained within the glass. At higher SA/V, the glass quickly approaches saturation levels for waste form corrosion products; thus, high SA/V tests are useful for mapping the rate at which a waste form corrodes during the interim stage of its reactions with water. Over the long term at high SA/V (or over shorter periods at extremely high SA/V), the solution becomes saturated with respect to waste form corrosion products, causing secondary crystalline phases to precipitate. Such tests provide information about the composition of the solution at saturation or, when no solution is recovered, the identities and order of appearance of secondary crystalline phases.

The test protocols adopted for testing Formula 127 and Formula 532 are designed to provide information about all three stages in waste form corrosion. Materials Characterization Center Type 1 (MCC-1) tests performed at low SA/V for 3, 7, and 16 d have been used to determine the relative reactivities of glass and the fluorite inclusions by monitoring F^- release to solution. Product Consistency Tests at much higher SA/V have been performed to measure the interim corrosion rate of both glass formulations. Argonne National Laboratory vapor hydration tests (VHT) performed at extremely high SA/V have been used to determine the identities and order of appearance of secondary crystalline phases. This information is used to model the long-term corrosion rate. Section II of this report describes the test methodology and the information obtained from each test; Sections III and IV describe the sample characteristics and test results for Formula 127 and Formula 532, respectively. The results are discussed in terms of the more general problem of the most appropriate methods for continued testing of LITCO waste glasses.

II. EXPERIMENTAL APPROACH

The test methodology involves reacting samples with water at elevated temperatures and variable SA/V. The tests employed in this effort are the MCC-1 test; the Product Consistency Test, Method B (PCT-B); and the Argonne VHT. The test matrices employed for Formula 127 and Formula 532 are shown in Tables 1 and 2, respectively. In the MCC-1 test, a monolith of a sample with a well-defined surface area is polished to 600 grit, then reacted with a volume of water such that the SA/V is 10 m^{-1}. The reference temperature is 90°C and the reference test duration is 28 d. At low SA/V and short reaction times, the reaction between solution and glass is dominated by the intrinsic durabilities of the glass and primary crystalline phases, because the solution remains dilute. The release of components to solution is expressed as the normalized elemental release, NL_i, defined as

$$NL_i = \frac{\text{concentration}}{f_i \bullet SA/V} \quad (1)$$

where f_i is the weight fraction of element i in the glass, and SA/V is the ratio of sample surface area to solution volume. The value of NL_i is therefore an estimate of the mass of glass that has reacted to produce the amount of the cation released to solution, and the maximum amount of glass that has reacted with solution is given by the element with the highest value of NL_i. Moreover, NL_i values for the components present in the highest concentrations in the glass indicate the mass of glass that has been dissolved. Several MCC-1 tests were performed on Formula 127 glass to investigate the relative reactivities of glass and primary crystalline phases in dilute solution, but it is known that even for very durable glasses the solution composition changes enough to affect reaction rates after 28 d at 90°C with SA/V = 10 m^{-1}. Shorter runs of 3, 7, and 16 d at 8.5 m^{-1} were performed to characterize the corrosion behavior in dilute solutions, as a complement to results obtained from PCT tests (discussed below).

Table 1. Test Matrix, Formula 127 Glass

Test Label	Test Type	SA/V, m^{-1}	Duration, d	Mesh Size	Status
W127-1	VHT	N.A.[a]	7	Monolith	Completed
W127-2	VHT	N.A.	14	Monolith	Completed
W127-3	VHT	N.A.	28	Monolith	Complete
W127-4	VHT	N.A.	56	Monolith	Completed
W127-5	PCT-B	2,000	7	-100+200	Completed
W127-6	PCT-B	2,000	70	-100+200	Completed
W127-7	PCT-B	2,000	140	-100+200	Completed
W127-8	PCT-B	20,000	28	-100+200	Completed
W127-9	PCT-B	20,000	TBD[b]	-100+200	TBD
W127-10	PCT-B	20,000	182	-100+200	November
W127-11	PCT-B	20,000	98	-100+200	October
W127-13	PCT-B	20,000	28	-200+325	Completed
W127-14	PCT-B	20,000	TBD	-200+325	TBD
W127-15	PCT-B	20,000	182	-200+325	November
W127-16	PCT-B	20,000	98	-200+325	October
W127-17	MCC-1	8.5	3	Monolith	Completed
W127-18	MCC-1	8.5	7	Monolith	Completed
W127-19	MCC-1	8.5	16	Monolith	Completed
W127-20	VHT	N.A.	112	Monolith	December

[a]Not applicable.
[b]To be determined.

Table 2. Test Matrix, Formula 532 Glass

Test Label	Test Type	SA/V, m^{-1}	Duration, d	Mesh Size	Status
W532-1	VHT	N.A.[a]	7	Monolith	Completed
W532-2	VHT	N.A.	14	Monolith	Completed
W532-3	VHT	N.A.	28	Monolith	October
W532-4	VHT	N.A.	56	Monolith	November
W532-5	PCT-B	2,000	7	-100+200	Completed
W532-5a	PCT-B	2,000	29	-100+200	Completed
W532-5b	PCT-B	2,000	49	-100+200	Completed
W532-6	PCT-B	2,000	70	-100+200	December
W532-7	PCT-B	2,000	140	-100+200	December
W532-8	PCT-B	2,000	TBD[b]	-100+200	TBD
W532-9	PCT-B	20,000	28	-100+200	October
W532-9a	PCT-B	20,000	49	-100+200	Completed
W532-10	PCT-B	20,000	98	-100+200	October
W532-11	PCT-B	20,000	182	-100+200	January 95
W532-12	PCT-B	20,000	98	-200+325	January 95
W532-13	PCT-B	20,000	182	-200+325	TBD
W532-14	PCT-B	20,000	TBD	-200+325	TBD
W532-15	VHT	N.A.	49	Monolith	Completed
W532-16	VHT	N.A.	98	Monolith	November
W532-17	PCT-B	20,000	7	-100+200	October

[a]Not applicable.
[b]To be determined.

The PCT-B method entails placing a mass of crushed glass of a particular size fraction in contact with deionized water and heating it at 90°C for various lengths of time. At the end of the test, the leachate solution is filtered to remove suspended glass particles and analyzed for solution concentrations of elements of interest. The sample surface area is estimated by assuming that the sample grains have some convenient shape, such as a sphere. On this basis, SA/V is 2000 m^{-1} for -100+200 mesh grains in contact with 10 times their mass of water, 20,000 m^{-1} for -100+200 mesh grains in contact with an equal mass of water, and 20,000 m^{-1} for -200+325 mesh grains in contact with twice their mass of water. These ratios have been used in PCT tests reported here. A departure from a symmetric distribution of particle sizes or changes in the surface roughness with changes in particle size will affect these estimates. The high SA/V values obtained in PCT tests provide a convenient means of accelerating saturation of a solution: the dissolution of a proportionally smaller amount of glass over a short period of time produces the same changes in solution composition as those produced in lower SA/V tests over much longer times. The PCT therefore highlights the effect that solution chemistry has on the corrosion of glass. Since the solution is concentrated with respect to glass corrosion products, the normalized mass loss to solution observed in PCT tests provides information about the interim rate of corrosion. If the test duration is long enough, the PCT can also provide information about secondary phase formation and long-term performance.

In the VHT, a monolithic sample is placed in contact with water vapor in a sealed vessel at elevated temperature. At relative humidities above ~90%, a thin film of water condenses on the sample, resulting in an extremely high SA/V and very rapid saturation of the solution with glass corrosion products. This results in rapid formation of secondary crystalline phases. Over time, the growth of secondary crystalline phases changes the composition of the solution, and the crystalline phases may enter into reactions with one another, producing a more stable phase

assemblage in the process. At the end of a test, the surface of the reacted sample is analyzed to identify the secondary crystalline phases that have formed and, if a well-defined alteration layer is present, to determine the rate of hydrolysis at the temperature at which the experiment was performed. The phases are identified by using analytical electron microscopy (AEM) or X-ray or neutron diffraction. The solution itself evaporates after the test is terminated, so solution analyses cannot be performed. The same phases are expected to form, and to have the same impact on corrosion rate, whether tests are performed at high or low temperature, thus, tests are generally performed at high temperature to accelerate corrosion

Vapor hydration tests can provide quantitative information about the rate of glass corrosion, but, more importantly, they also provide qualitative information about the identities and order of appearance of secondary crystalline phases. These factors are potentially important to the long-term corrosion rate, for if the rate of crystal growth exceeds the rate of glass corrosion in the absence of the crystal, then the rate of corrosion may accelerate when the crystal is present. This information is essential for long-term modeling of glass performance. On the basis of past experience, VHT tests were performed at 200°C for test durations of 7 to 56 d.

III. RESULTS: FORMULA 127

A. Sample Characteristics

Formula 127 is a translucent green glass. While mostly translucent in bulk, when seen in transmitted light, thin slabs of Formula 127 show patches of greater transparency 1-4 mm in diameter. In backscatter electron images one can clearly see bright patches indicative of heterogeneities in bulk composition. The heterogeneities have been shown by energy dispersive spectroscopy (EDS) to be nearly pure CaF_2, and they are assumed to be the mineral fluorite. Most of the fluorite takes the form of flower-shaped spherulites 2.5 μm in diameter that are distributed 5-15 μm apart (Fig. 1). The cores of the spherulites are pure fluorite, but the "petals" are interpenetrated with glass. Fluorite also takes the form of large, skeletal masses up to 5 mm in diameter. In cross section, the volumes of these pseudomorphs are seen to consist almost entirely of glass, penetrated by dendritic intergrowths of fluorite. The small, spherulitic fluorite crystals are entirely absent from the regions of dendritic fluorite crystals, as seen in the backscatter image in Fig. 2. No other crystalline phases have been found in images obtained by scanning electron microscopy (SEM), though a very small number of 50-100 μm opaque particles have been observed in thin sections of the glass. The identity of these particles has not been determined as yet.

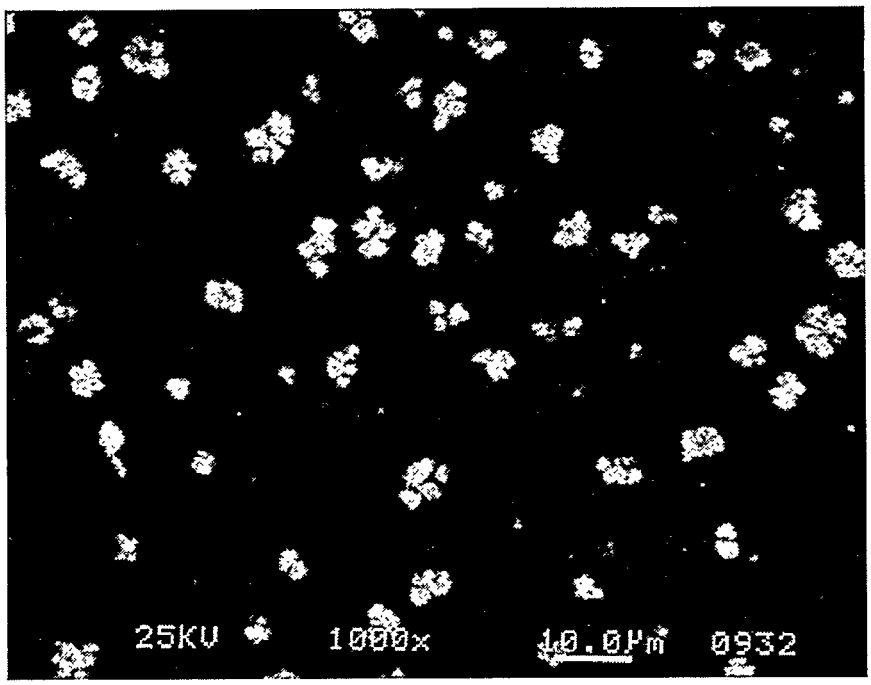

Fig. 1. Backscatter Image of a Polished Surface of Formula 127. Irregular white patches are spherulitic "flowers" of CaF_2 or fluorite. Magnification is 1000X.

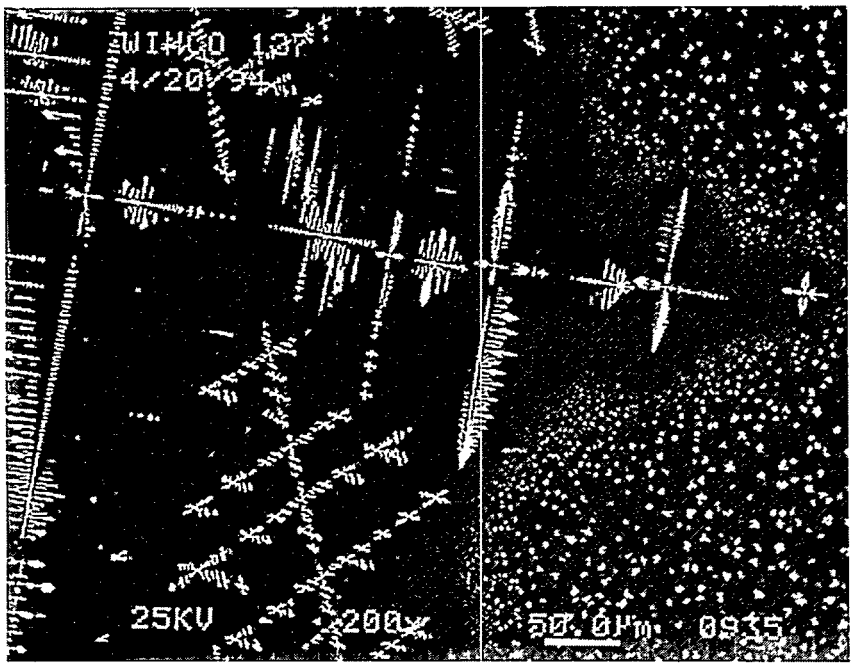

Fig. 2. Backscatter Image of a Polished Surface of Unreacted Formula 127, Showing Dendritic Fluorite Crystals (Long, Bladed Features) and Spherulitic Fluorite (Small White Patches). The glass surrounding the crystals is depleted in Ca and F relative to the bulk. Magnification is 200x.

The composition of Formula 127 given by Staples et al. [1], is reproduced in Table 3. We have also recast the composition in terms of oxide and fluoride components. This representation shows that all calcium can be accounted for by a CaF_2 component, part of which is dissolved in the glass and part of which is present in fluorite crystals. The fluoride that is not accounted for by calcium has been arbitrarily assigned to the glass component NaF. The high fluoride concentration of the glassy part of Formula 127 has no counterpart in any candidate high-level vitreous waste forms. The composition of Formula 127 is also unusual in that the B_2O_3 concentration is much lower than in most high-level waste glasses, and the ZrO_2 concentration is much higher than in most waste glasses. At low concentrations, B_2O_3 does not strongly affect durability either way, and ZrO_2 is believed to improve the durability of alkali borosilicate glasses [2]. The relatively low alkali concentration and relatively high Al_2O_3 concentration is consistent with the good performance of Formula 127 in short-term leach tests reported by Staples et al. [1].

The composition of Formula 127 glass was analyzed using semiquantitative EDS on an electron microprobe and a wide (500 µm x 500 µm) raster. The results were in good agreement with the reported analyses. A more tightly focused raster (5-10 µm in diameter) was used to analyze the interstitial glass between fluorite grains (the dark areas in Figs. 1 and 2). This glass was depleted in Ca and F relative to the bulk. Fluorite is estimated to comprise approximately 5-10% of the bulk material.

Table 3. Bulk Composition of Formula 127 Glass

	Elements[a]		Oxide and Halide Components[b]		
Component	at %	wt %	Component	mol %	wt %
Al	4.1	5.08	Al_2O_3	6.1	9.2
B	1.3	0.65	B_2O_3	1.9	2
Ca	5.2	9.57	CaF_2[c]	17.3	20.0
Cu	0.6	1.75	CuO	1.8	2.1
Li	3.6	1.15	Li_2O	5.4	2.4
Na	4.1	4.33	Na_2O	4.3	4.0
Si	18.2	23.47	NaF[c]	3.6	2.2
Zr	1.8	7.54	SiO_2	54.2	48.3
F	11.6	10.12	ZrO_2	5.4	9.8
O	49.5	36.36			

[a]Data from Staples et al. [1].
[b]Elemental composition reported by Staples et al. [1] converted to oxide/halide composition.
[c]Assumed components required to balance fluoride in bulk analysis.

B. Test Results

The Argonne VHT tests on the original test matrix (Table 1) were run for 7, 14, 28, and 56 d. An additional test has been started that will run for 112 d to verify the secondary phase assemblages seen in the 56-day test. The PCT-B tests run for 7, 70, and 140 d with SA/V = 2000 m^{-1}, and for 28 d at 20,000 m^{-1} have been completed. Tests at 20,000 m^{-1} for 98 and 182 d will be terminated in October and November 1994, respectively. Solution analyses for cations have been obtained from all PCT tests terminated thus far. Solution analyses for fluorine have been obtained for tests W127-6, W127-8, and W127-13. We have also performed MCC-1-type experiments at SA/V = 8.5 m^{-1} for test durations of 3, 7, and 14 d in an effort to determine the forward rate of glass corrosion and for comparison with the results reported by Staples et al. [1]. Solution analyses for cations have been obtained for all MCC-1 tests, and fluorine analyses have been obtained for tests W127-17 and W127-18.

1. Materials Characterization Center Type-1 Test Results

Table 4 shows the pH and elemental concentrations of solutions obtained from MCC-1 tests W127-17, W127-18, and W127-19. Solution concentrations of major cation components were analyzed using inductively coupled plasma-mass spectrometry (ICP-MS). Reported uncertainties are ±15% for most elements (higher uncertainties were reported for calcium due to the coincidence of the masses of ^{40}Ca and ^{40}Ar). Fluorine analyses were performed by ion chromatography (IC) and have an estimated uncertainty of 5%. Table 5 shows normalized releases for each element as obtained from these tests. These decrease in the order

Table 4. Formula 127, MCC-1 Solution Compositions, ppm

Test No.	W127-17	W-127-18	W127-19
Test Type	MCC-1	MCC-1	MCC-1
Duration, d	3	7	16
SA/V, m^{-1}	8.5	8.5	8.5
Final pH	7.72	7.69	7.74
Analysis Method	ICP-MS	ICP-MS	ICP-MS
Al	0.64	0.78	0.91
B	0.55	0.63	0.74
Ca	2.2	2.9	3.1
Cu	0.032	0.034	0.030
Li	0.68	0.77	0.91
Na	2.4	2.7	3.4
Si	7.7	9.2	11
Zr	0.002	0.002	0.006
Analysis Method	IC	IC	
F	2.2	3.5	

Table 5. Formula 127, MCC-1 Normalized Release, g/m^2

Test No.	W127-17	W-127-18	W127-19
Test Type	MCC-1	MCC-1	MCC-1
Duration, d	3	7	16
SA/V, m^{-1}	8.5	8.5	8.5
Final pH	7.72	7.69	7.74
Al	1.5	1.8	2.1
B	10	11	13
Ca	2.8	3.5	3.8
Cu	0.22	0.23	0.20
Li	7.0	7.9	9.3
Na	6.4	7.4	9.4
Si	3.9	4.6	5.6
Zr	0.002	0.003	0.009
F	2.6	4.1	

B > Li, Na > Si > F > Al >> Cu >> Zr. The maximum normalized release, 10 g/m^2, was obtained for B in the 3-d test (W127-17), and implies a normalized mass loss rate of 3.3 $g/m^2/d$. The bulk of the mass actually lost from the waste form, however, results from removal of Si, Na, Li, and F, which have normalized elemental release rates of 1.3, 2.2, 2.3, and 0.9 $g/m^2/d$, respectively. After 16 d, the rate of mass loss (based on sodium) decreased to 0.6 $g/m^2/d$, showing that even at the very low SA/V of these tests, the changes to solution chemistry produced by glass corrosion have already affected the corrosion rate.

2. Product Consistency Test: Solution Analyses

Cation concentrations in solutions from tests W127-5, W127-6, W127-8, and W127-13 were analyzed using inductively coupled plasma-atomic emission spectroscopy (ICP-AES), and those from test W127-7 were analyzed using ICP-MS. Fluorine analyses were obtained using IC. Table 6 shows the pH and elemental concentrations of solutions obtained from PCT-B tests, and normalized elemental releases are shown in Table 7. Uncertainties are the same as those for the MCC-1 solution analyses.

Table 6. Formula 127, MCC-1 Solution Compositions, ppm

Test No.	W127-5	W-127-6	W127-7	W127-8	W127-13
Test Type	PCT-B	PCT-B	PCT-B	PCT-B	PCT-B
Duration, d	7	70	140	28	28
SA/V, m^{-1}	2,000	2,000	2,000	20,000	20,000
Final pH	9.93	10.02	9.21	10.92	11.13
Analysis Method	ICP-AES	ICP-AES	ICP-MS	ICP-AES	ICP-AES
Al	<1.3	<1.0	1.01	<2.0	<1.4
B	6.9	8.6	6.4	24	29
Ca	4.4	3.2	4.1	1.2	1.4
Cu	<0.1	<0.1	0.004	<0.2	<0.1
Li	11	16	15	48	58
Na	30	41	38	120	140
Si	36	42	53	91	110
Zr	<0.3	<0.2	0.001	<0.4	<0.3
Analysis Method		IC	IC		IC
F		21	69		71

Table 7. Formula 127, PCT-B Normalized Elemental Release, g/m^2

Test No.	W127-5	W-127-6	W127-7	W127-8	W127-13
Test Type	PCT-B	PCT-B	PCT-B	PCT-B	PCT-B
Duration, d	7	70	140	28	28
SA/V, m^{-1}	2,000	2,000	2,000	20,000	20,000
Final pH	9.93	10.02	9.21	10.92	11.13
Al	<0.013	<0.01	0.010	<0.002	0.001
B	0.54	0.67	0.50	0.18	0.22
Ca	0.023	0.017	0.021	0.001	0.001
Li	0.48	0.69	0.63	0.21	0.25
Na	0.34	0.47	0.44	0.13	0.16
Si	0.077	0.089	0.11	0.019	0.023
F		0.10		0.034	0.035

In the 2000 m^{-1} PCT-B tests, the normalized releases decrease in the order Li, B > Na > F > Si > Ca >> Al. The normalized releases for Al, Cu, and Zr are below the limits of detectability in the ICP-AES analyses, consistent with the very low releases obtained for these elements in the ICP-MS analysis. The concentrations of Ca and Si increase from 70 to 140 d, but the concentrations of other components decrease with time. The final pH of W127-7 is lower than that obtained for any other PCT-B test and is consistent with the lower normalized mass losses observed for most elements in this test. The normalized elemental releases are on the order of 0.4-0.7 g/m^2 for the most soluble glass components (Li, B, and Na).

The 28-d PCT tests, W127-8 and W127-13, were performed at SA/V of 20,000 m^{-1}, but test W127-8 was performed with a -100+200 sieve fraction and W127-13 with a -200+325 sieve fraction. The solution concentrations of all glass components are much greater in these tests than in the 2000 m^{-1} tests, illustrating the pronounced effect that SA/V has upon solution chemistry. Normalized elemental releases and the final pH for W127-8 are consistently lower than those obtained for W127-13, though in general the agreement between the two tests is fairly good. The normalized release of the glass components varies in the same order in the high and low SA/V tests; however, the normalized releases of Na and Si are lower relative to those for Li and B in the tests at 20,000 m^{-1}. This discrepancy is even greater in the case of Ca. The overall normalized release rates are much lower for the 20,000 m^{-1} tests than might be expected from the 2000 m^{-1} tests because dissolution of a much smaller quantity of glass is needed to bring the concentration of components in solution near the saturation level.

3. Product Consistency Test: Sample Analyses

After termination of a test, the PCT samples were washed three times with deionized water to remove any components from the interstitial fluid that might precipitate as an evaporite layer on the surface of the grains. As a precaution, small amounts of glass were removed before washing to verify that no very small secondary crystalline phases were washed away. Analysis of the washed and unwashed PCT samples by SEM showed that no silicate secondary crystalline phases were formed in the tests terminated thus far. However, there is evidence that fluorite grains actually grow during the course of the tests. The grains of freshly crushed Formula 127 are smooth, with fluorite crystals apparently cleaving parallel to the glass surface as the glass fragments. In the PCT samples, however, most fluorite grains protrude above the surface of the glass, and most are also surrounded by small depressions indicative of selective dissolution of the glass. An example is shown in Fig. 3, which is an SEM image of the surface of a glass grain taken from test W127-6, the 70-d PCT test at 2000 m^{-1}. In the 140-d PCT samples the fluorite grains acquire relatively well-defined crystal faces. This observation and the low calcium concentrations in solution suggest that as calcium is removed from the bulk glass some of it reprecipitates as CaF_2 crystals.

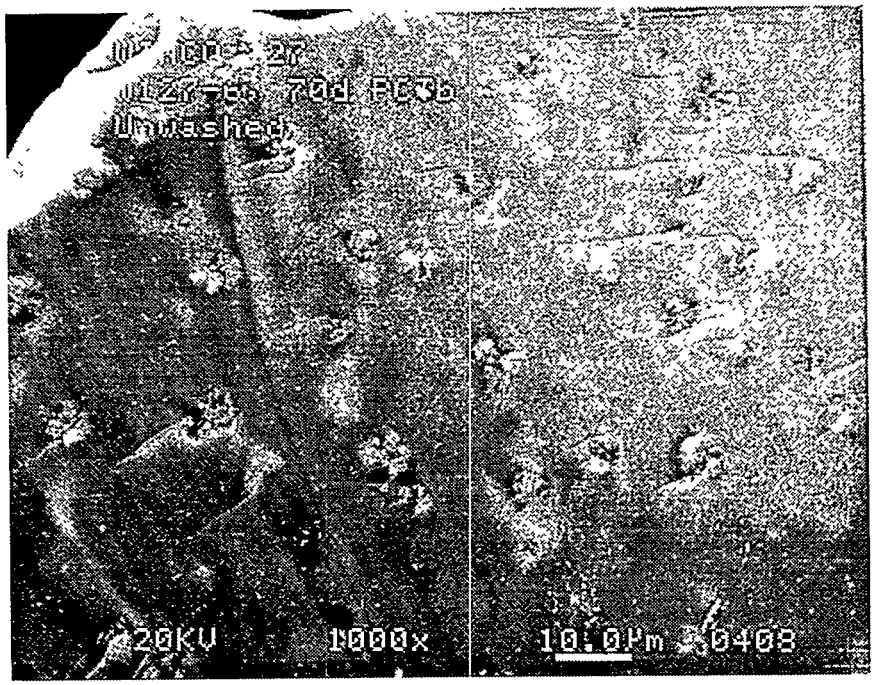

Fig. 3. SEM Image of the Surface of a Grain Taken from a 70-d, 2000 m^{-1} PCT-B Test of Formula 127. The small, irregular features are primary fluorite crystals that protrude above the surface of the glass. The smooth curves sweeping from the bottom to the top of the picture are conchoidal fractures producedwhen the sample was crushed for the test. Magnification is 1000X.

Grain mounts have been made of all samples from PCT tests conducted for Formula 127. These mounts allow cross-sectioning of grains and an analysis of the depth of aqueous attack. An estimate of the depth of hydration can be obtained by dividing the normalized mass loss of the component with the highest release rate by the density of the sample. This calculation provides an equivalent depth of total extraction of the component in question in micrometers. The maximum normalized release is approximately 0.7 g/m^2, and if the bulk density is assumed to be 2.7 g/cm^3, the extraction depth is 0.27 μm for B release, and less than half this for the more important glass components Na and Si. This distance is too thin to resolve by SEM, and therefore it is not surprising that no evidence of a reacted layer is seen in any of the PCT tests terminated thus far for Formula 127. The estimate of surface layer thickness is well within the detection limits of AEM, and PCT samples have been submitted for AEM analyses.

An interesting result seen in cross-sectioned PCT samples is that individual grains disintegrate somewhat about their borders. The depth to which disintegration extends varies directly with the duration of the experiment, though in a qualitative rather than quantitative way. Most grains from W127-7 showed evidence of breakage throughout their entire volume. On the other hand, cross sections taken through the unreacted glass were clean, with no disruption to the surface of the grains. This suggests that the outer layers of the glass have been embrittled by reaction with water. On the basis of the VHT test results discussed below, it is suggested that there is extensive percolation of water into the bulk glass, possibly through hydroxyl exchange for fluoride.

To summarize, analysis of solids removed from PCT tests show that for the tests completed thus far, no secondary silicate crystalline phases have formed. Calcium that dissolves during glass corrosion may reprecipitate on exposed fluorite grains. Unfortunately, such precipitation is very difficult to determine from PCT tests because it is impractical to monitor the behavior of a single grain of material.

4. Vapor Hydration Test Results

The purpose of the ANL VHT is to greatly accelerate the corrosion progress and hasten the formation of secondary phases. When a glass forms a well-defined alteration layer, the thickness of the layer can also be used to gauge the rate of glass reaction with water vapor. Formula 127 does not form an alteration layer thick enough to resolve with an SEM, so samples have been submitted for analysis by transmission electron microscopy. As with the PCT test samples, however, cross-sectioning of VHT samples results in partial disintegration of the material near the surface of the monoliths, indicating that the reacted glass is more fragile than the unaltered glass. Furthermore, in a recent reexamination of VHT samples that were sealed in epoxy several months ago, we found that all samples had pulled back from the epoxy over time, leaving a gap around the periphery of the monoliths. The width of this gap and the degree of disruption of the surface of the glass produced by polishing the samples increased with the duration of the hydration test, though as with the PCT test, this greater fragility is simply a qualitative indication of extensive hydration of the sample. In the most extreme case, the contraction was nearly 20 μm around the entire monolith, indicating a 3-4% volume contraction over time. This contraction provides further evidence that Formula 127 is extensively infiltrated with water in hydrothermal tests. Depending on how much fluoride is exchanged out of the bulk glass in this process, hydrolysis might change the bulk chemistry of the glass enough to influence its corrosion behavior. This point is addressed in greater detail in Section V.

The first phases to appear in VHT tests are calcium silicates, one with a Ca:Si ratio near 1:1 and another with a Ca:Si ratio >2:1. A crystal rich in Si, O, and F also forms early in the hydration tests, but the possibility that Li or B might also be present cannot be excluded. A phase apparently containing Ca and O alone also forms, but it is so irregular in shape and so low in concentration that it may be $Ca(OH)_2$ precipitated as an evaporite. At longer times, the

Ca:Si phase with high calcium concentration disappears, and the phase with Ca:Si of 1:1 appears to be in a reaction relationship with $CaCO_3$, calcite. Figure 4 shows a $CaCO_3$ crystal growing around an interior calcium silicate, found on the surface of a monolith exposed to water vapor for 28 d. The predominant calcium-bearing phase thereafter is calcite, which grows to 50-100 μm in diameter after 56 d. Zirconium also appears in secondary crystalline phases, in a Ca-Zr-F phase (possibly $CaZrF_6$) and in a Ca-Zr-Si-O-F phase. Silicon is concentrated mainly in the latter secondary phase. There are a few grains of Na-Al silicate, which because of its relatively poorly developed crystal phases is probably a feldspar (e.g., $NaAlSi_3O_8$). All secondary crystalline phases will be quantitatively identified by AEM analysis.

Though these phases are widespread and, in the case of $CaCO_3$, grow to nearly macroscopic size, the glass itself does not appear to undergo very extensive corrosion. In other words, a relatively small amount of glass is reacting to form the phases observed in the VHT tests. This suggests that the phases formed thus far are not likely to have a very substantial impact on the long-term rate of glass corrosion and perhaps on the release rate of radionuclides. A more definitive answer will come from the long-term PCT tests currently underway.

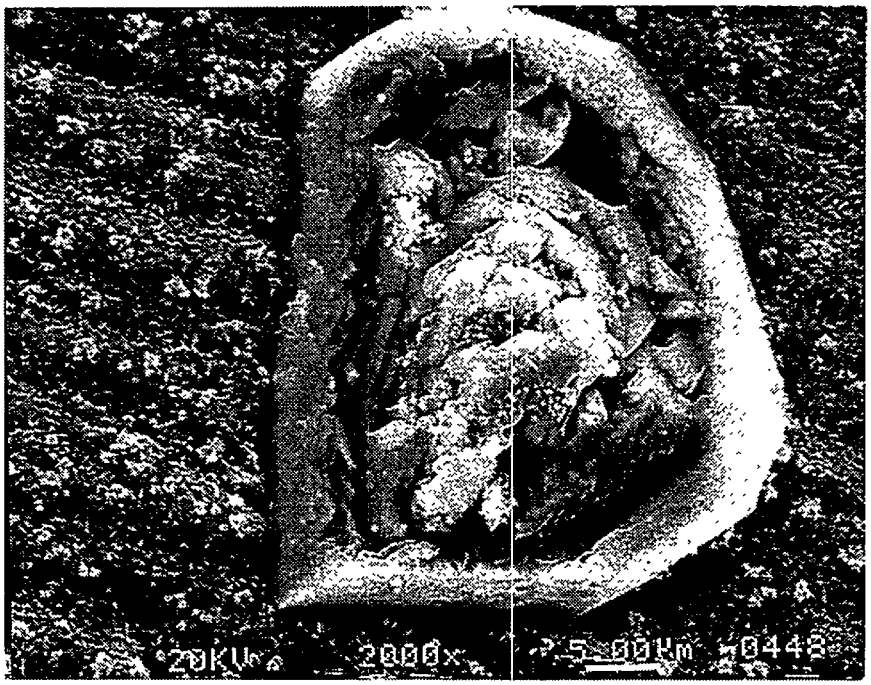

Fig. 4. SEM Image of a Secondary Crystalline Phase Produced during a 28-d VHT of Formula 127. The image shows a ring of $CaCO_3$ (calcite) growing around and reacting with a central crystal of calcium silicate. The background material is an altered clay layer. Magnification is 2000X.

IV. RESULTS: FORMULA 532

A. Sample Characteristics

Formula 532 was received in the alumina crucible in which it was formed. After a crust near the surface of the glass (mainly Al_2O_3) was broken off, the remainder of the glass was easily removed from the crucible. This indicates that the melt had not wetted the crucible. Formula 532 is a transparent, deep-blue glass with swirls of much darker glass in places and relatively large (1-5 μm) blobs of light-colored undissolved or partially reacted material. Measurements by EDS of the partially reacted material indicate that its composition is similar to that of the bulk glass, though depleted somewhat in Na (and presumably in the fluxes Li and B as well). Images obtained by SEM of crushed glass reveal that 5-10% of the bulk material is a crystalline phase with an EDS spectrum consistent with equal atomic concentrations of Al and Si. No binary aluminosilicate minerals have an Al:Si ratio of 1:1, so a light element such as Li or B must be present as a principal component but was not detected by EDS. Lithium is a likely candidate, in which case the probable identity of the crystalline phase is β-eucryptite, $LiAlSiO_4$. The crystals in the crushed sample do not have regular crystal faces, as would be expected from a phase in equilibrium with the melt, but they also do not have the morphology of quench crystals, which indicates that the crystals seen in the crushed sample are fragments of still larger crystals. This implies that crystals in excess of 100 μm in diameter exist in the parent glass. A detailed examination of the glass was not performed prior to crushing and cutting monoliths, but in retrospect such an examination might have helped to determine whether the crystals had settled to the bottom of the alumina crucible.

The crystalline phase and bulk glass have nearly the same average atomic number, so it is very difficult to distinguish between them in electron backscatter images. Because the crystal has a different intrinsic electron conductivity, however, it does appear somewhat different from the glass in regular SEM images. The surfaces of Formula 532 monoliths and glass fragments appear to be covered with 1-2 μm crystals with similar contrast in SEM images, though they are too small to yield reliable EDS spectra. These may be the same crystal phase. If this is so, it might explain the appearance of phases observed in VHT tests (see below).

The composition of Formula 532 was supplied with the glass and is reported in Table 8 in terms of weight percent of oxide components and atom percent of elements. One of the components in the glass is referred to as "alumina calcine," but because its composition was not provided, we have assumed that it is pure Al_2O_3 both in Table 8 and in calculating normalized release rates. To the extent that other cations are present, the normalized release for Al_2O_3 will increase and the release of other cations will decrease. In this approximation, the composition of Formula 532 is unique in its high Al_2O_3 concentration: the only candidate waste glass we have identified with a comparable Al_2O_3 concentration is SAN 60 [3] which has a comparably high alkali oxide concentration but a much higher B_2O_3 concentration.

B. Test Results

Testing of Formula 532 samples started in July 1994, so fewer tests have been completed than for Formula 127. The ANL VHT tests in the original test matrix (Table 2) were run for 7, 14 and 49 d. A 98-d VHT has been included in the test matrix. The PCT-B tests were run for 7, 28, and 49 d at a SA/V = 2000 m^{-1} and for a duration of 49 d at 20,000 m^{-1}. Solution analyses for cations have been obtained from all PCT tests terminated thus far. No MCC-1 tests were performed on this glass.

Table 8. Bulk Composition of Formula 532 Glass

Elements			Oxide Components		
Component	at. %	wt %	Component	mol %	wt %
Al	7.95	11.64	Al_2O_3 [a]	13.7	22.0
B	5.34	3.14	B_2O_3	9.2	10.1
Cu	0.46	1.60	CuO	1.6	2.0
Li	8.75	3.30	Li_2O	15.1	7.1
Na	4.22	5.27	Na_2O	7.3	7.1
Si	14.28	21.78	SiO_2	49.2	46.6
Ti	1.18	3.06	TiO_2	4.0	5.1
O	57.81	50.22			

[a]Weight is for alumina calcine, assumed to be pure Al_2O_3.

1. Product Consistency Test: Solution Analyses

Solution pH and cation concentrations obtained from PCT solution analyses are shown in Table 9, and normalized elemental releases for the cations are shown in Table 10. Because tests on Formula 532 started much later than those for Formula 127, the data set is smaller and consists largely of relatively short-term tests. These results are probably not sufficient to provide significant conclusions about the performance of Formula 532 under hydrothermal conditions. The normalized release for B is the greatest of any element, followed by Li, Na, Al and Si. The release for Al is much greater than that observed for other candidate waste glass compositions, such as Formula 127 (Table 7). The normalized release of Al, B, Cu, and Li increases over time, but the normalized release of Na and Si decreases from the 29-d to the 49-d PCT-B tests conducted at SA/V = 2000 m^{-1}. The decline may be due to the formation of zeolite observed in the 49-d PCT samples, as discussed below. On the whole, normalized releases appear to be comparable to those observed for Formula 127 for all elements except B and Al.

2. Product Consistency Test: Sample Analyses

After 49 d at 20,000 m^{-1}, Formula 532 samples exhibit secondary crystalline phases: a cubic Na-Al-Si phase with a Na:Al atomic ratio of 1:1, tentatively identified as a zeolite, and very small crystals with Ti:Al atomic ratio of 1:2 that are probably $TiAl_2O_5$. It is impossible to tell in these tests whether the Al-Si primary phase has accreted material from the solution, but results from the VHT tests (see below) indicate that this is to be expected. For reference, SAN 60 [3] has relatively low release rates in static leach tests at low SA/V (10-100 m^{-1}), but after 28 d tests at 100 m^{-1} and 150°C, the surface of SAN 60 grains are completely coated with zeolites and hydrous lithium aluminosilicate crystals ($LiAlSiO_4 \cdot 2H_2O$). The comparatively high Al_2O_3 and Li_2O concentrations of Formula 532 make it likely that a similar lithium aluminosilicate crystal forms during its corrosion, perhaps on the surface of the Al-Si-rich primary crystalline phase.

Table 9. Formula 532, PCT-B Solution Concentrations, ppm

Test No.	W532-5	W532-5a	W532-5b	W532-9a
Test Type	PCT-B	PCT-B	PCT-B	PCT-B
Duration, d	7	29	49	49
SA/V, m^{-1}	2.000	2,000	2,000	20,000
Final pH	9.51	9.61	9.41	9.68
Analysis Method	ICP-MS	ICP-MS	ICP-MS	ICP-MS
Al	47	54	55	32
B	83	84	92	817
Cu	1.7	2.4	2.7	0.1
Li	45	53	57	440
Na	50	38	37	245
Si	81	96	88	52
Ti	ND[a]	ND	ND	ND

[a]No data.

Table 10. Formula 532, PCT-B Normalized Release, g/m^2

Test No.	W532-5	W532-5a	W532-5b	W532-9a
Test Type	PCT-B	PCT-B	PCT-B	PCT-B
Duration, d	7	29	49	49
SA/V, m^{-1}	2.000	2,000	2,000	20,000
Final pH	9.51	9.61	9.41	9.68
Al	0.20	0.23	0.24	0.01
B	1.32	1.34	1.47	1.30
Cu	0.05	0.08	0.09	0.00
Li	0.68	0.80	0.86	0.67
Na	0.47	0.37	0.35	0.23
Si	0.19	0.22	0.20	0.01
Ti	ND[a]	ND	ND	ND

[a]No data.

3. Vapor Hydration Test Results

After 7 d at 200°C, Formula 532 shows an alteration layer with an average thickness of 30 μm, with occasional penetrations as deep as 50 μm. The alteration layer consists of altered glass that very easily flakes off the monolith. Figure 5 is a 1000X SEM image showing the surface of the altered glass layer. The layer is filled with trapezoidal 1-4 μm crystals that have EDS spectra identical to those of the Al-Si primary crystalline phase. The deep pit in the center of Fig. 5 is also a characteristic feature of the altered layer of the 7-d VHT sample. Isolated Na-Al-Si crystals were also identified, though their volume is much less than that of the Al-Si-rich alteration phases. After a 14-d VHT at 200°C, the surface of Formula 532 is extensively altered, with a depth of alteration/recrystallization of approximately 120 μm. Figure 6 is a 200x SEM image of the surface of a sample resulting from test W532-2. The surface is almost entirely coated with spherulitic masses of an Al-Si-rich phase with an EDS spectrum identical to that of the Al-Si-rich primary phase. These are the columnar, radiating crystals in Fig. 6. The large, faceted, almost spheroidal crystal in the center of Fig. 6 is a zeolite crystal. Several of the zeolite crystals are more than 1 mm in diameter. The dark area in Fig. 6

that appears free of crystals is the glass surface that has been altered to clay. No new phases are evident after 49 d at 200°C (test W127-3A). Figure 7 is an SEM image of a cross section taken through a sample from test W127-3A. The thickness of the alteration layer has increased to an average of approximately 300 μm, with pockets of penetration as deep as 400 μm. The surface layer is composed almost entirely of the Al-Si-rich phase. This is underlain by a Na-rich, Al-depleted material, which is in turn is underlain by an Al-Si-rich phase, but one containing 1-2 wt % Ti as well. This is again underlain by a Na-rich, Al-depleted material. This pattern is repeated several times, with the last Na-rich, Al-depleted layer underlain by a material with an EDS spectrum identical to the unaltered glass.

Formula 532 obviously reacts very quickly under vapor-saturated conditions at 200°C, because the samples reacted for 7 d were already in a relatively advanced stage of corrosion. For this reason, it is important to verify that the reaction mechanism does not change as a function of temperature. Tests were performed at 200°C on the basis of past experience with durable waste glasses. It may be necessary to perform VHT tests at lower temperatures to confirm that the same phases are obtained and to examine the very early stages of the reaction of Formula 532 with water vapor.

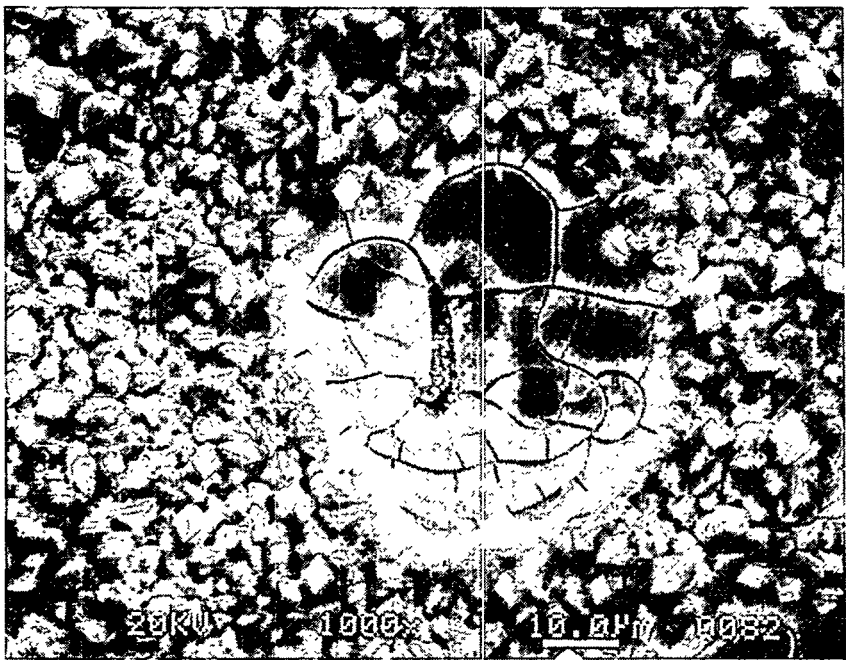

Fig. 5. SEM Image of the Surface of a 7-d VHT Sample of Formula 532. The small white trapezoidal features are an Al-Si-rich secondary phase with an EDS spectrum identical to the primary crystalline phase. An etch pitch is in the center of the image. Through the crack in the bottom of the etch pitch one can see an underlying alteration layer is visible. Magnification is 1000X.

Fig. 6 SEM Image of the Surface of a 14-d VHT Sample of Formula 532. The large, multifaceted, spheroidal crystal in the center of the image is a Na-Al-Si phase, presumably a zeolite. The bladed crystals growing in bundles are the same Al-Si-rich phase seen in Fig. 5. The background material is an altered clay layer. Magnification is 500X.

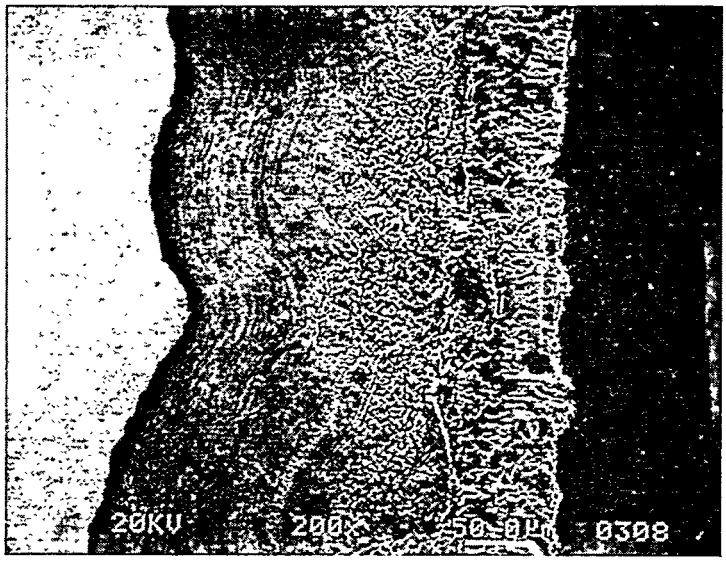

Fig. 7 SEM Image of a Cross-Section of a 49-d VHT Sample of Formula 532. The alteration layer is the dark band in the center of the image. The light material at the left is unaltered glass. Layers that consist almost entirely of the Al-Si-rich phase (i.e., the phase in Figs. S 5 and 6) are identified as "A," whereas those that consist of a Na-rich, Al-depleted material are identified as "N." The layer in contact with the unaltered glass is "N." The large relief between the alteration layer and the unaltered glass is due to the reduced mechanical strength of the alteration layer. Magnification is 200X.

V. CONCLUSION

Table 11 compares the 7-d PCT results NL_{Na} for Formula 127 and NL_B for Formula 532 with the 7-d NL_B for several waste glasses. The value for NL_{Na} is used for Formula 127 because of the very low B concentration of that glass. The normalized mass loss of Formula 127 is comparable to that of HW-39, SRL 202U, and WV 6, the reference waste forms for the U.S. Department of Energy's Hanford site, Savannah River Laboratory, and the West Valley Demonstration Project, respectively. No secondary crystalline silicate phase has been observed in the PCT test completed for Formula 127 thus far, but VHT results indicate that a complex assemblage of fluoride phases is to be expected. The relatively low release rates for Formula 127 indicate that it is a durable waste form. The NL_B value for Formula 532 is higher, falling between the values obtained for these glasses and for SRL EA. The rate of release of other glass-forming components from Formula 532 is also relatively high, particularly for aluminum. Formula 532 is thus a moderately durable glass, but early results indicate that the low release rates may be caused partly by glass components in solution reprecipitating on growing crystals of an Al-Si-rich primary crystalline phase and secondary zeolite phases. Secondary phases formed in VHT tests consist almost entirely of a zeolite and an Al-Si-rich crystal that has an EDS spectrum similar to the primary phase. Primary phases are being identified using neutron diffraction analysis, and secondary crystalline phases obtained in VHT tests and PCT tests will be analyzed by AEM.

The test results indicate that at a minimum the primary crystalline phases influence the chemistry of the solution, and it is possible, in the case of Formula 532, that they exert control over glass dissolution. In the case of Formula 127, PCT solutions analyzed thus far have not evolved enough to precipitate secondary crystalline phases, but VHT tests indicate that fluoride-bearing phases should be expected. This suggests that the main role of secondary crystalline phases will be to accommodate fluoride, and therefore these phases may not influence the rate of glass dissolution. Longer VHT tests may indicate whether aluminosilicate crystals form in the long term. If the interpretation that calcium precipitates onto existing fluorite grains proves correct, then the presence of fluorite grains on the glass surface exerts a controlling influence on the solution concentrations of calcium and to some extent on fluorine as well. In this sense, fluorite behaves both as a primary phase and as a secondary crystalline phase. The fluorite in the glass matrix and the secondary phases formed in very high SA/V tests do not appear to negatively affect the rate of corrosion of Formula 127.

The Al-Si-rich primary crystalline phase in Formula 532 also appears to be an early-forming secondary crystalline phase during glass corrosion, along with a zeolite phase. Long-term solution data are expected to indicate the extent to which these crystals affect the rate of glass dissolution. The VHT results indicate that an Al-Si-rich crystalline phase and a zeolite phase are the most important secondary corrosion products for Formula 532, and that a large fraction of the total mass of the glass is converted to these phases as corrosion proceeds. It is

Table 11. Seven-Day PCT NL_B and NL_{NA} for Formula 127 and NL_B for Formula 532 Compared with 7-d PCT NL_B for other Waste Forms

Name	NL_B, g/m^2	Nl_{Na}, g/m^2
Formula 127	0.5	0.3
Formula 532	1.4	
HW-39	0.4	
SRL 202U	0.4	
SRL EA	5.0	
WV 6	0.3	

anticipated that these phases will form in long-term PCT tests and may accelerate the reaction rate in the long term. In this case, Formula 532 will not perform as well as Formula 127 in long term PCT tests.

While secondary crystalline phases are thermodynamically more stable than the glass, the glass must break down to form them, and any components that are not soluble in the secondary phases can potentially be released to solution. It is anticipated that long-term PCT tests and VHT tests will shed more light on this issue, but better tracking of the appearance of secondary phases may be required to accurately assess the performance of these glasses. This is particularly important in the case of radionuclides, which will be distributed among the glass, primary crystalline phases, solution, and secondary crystalline phases. Furthermore, breakdown of the glass into secondary crystalline phases that do not incorporate radionuclides will result in the release of radionuclides into the environment. The distribution of radionuclides and the rate of their release can only be determined by evaluating radioactive glasses, preferably glasses containing actual waste materials.

ACKNOWLEDGMENTS

The authors wish to thank Jeff Emery for preparing sample materials for testing, and Norma Barrett for assistance in preparing the manuscript for publication. We also wish to thank William Ebert for technical advice during the course of this project and for helpful comments on the manuscript.

This work supported by the U.S. Department of Energy, Lockheed Idaho Technologies Company, under contract DE-AC07-94ID13223.

REFERENCES

1. B. Staples, H. Cole, and D. Pavlica, "Properties of Formula 127 Glass Prepared with Radioactive Zirconia Calcine," *Mat. Res. Soc. Symp. Proc.* 15, 125-134 (1983).

2. X. Feng, Aa. Barkatt, and T. Jiang, "Systematic Composition Studies of the Durability of Waste Glass WV205," *Mat. Res. Soc. Symp. Proc.* 112, 543-554 (1988).

3. *Testing and Evaluation of Solidified High Level Radioactive Waste*, A. R. Hall, ed. Graham & Trotman, London, p. 10 (1987).

Distribution for ANL-95/12

Internal:

J. K. Bates (35)
J. C. Cunnane
A. J. G. Ellison
J. E. Harmon
J. E. Helt
J. Laidler
C. C. McPheeters
J. G. Peak
S. F. Wolf
TIS Files

External:

DOE-OSTI (2)
ANL-E Library (2)
ANL-W Library
Manager, Chicago Operations Office, DOE
A. Bindokas, DOE-CH
J. Haugen, DOE-CH
Chemical Technology Division Review Committee Members:
- E. R. Beaver, Monsanto Company, St. Louis, MO
- D. L. Douglas, Consultant, Bloomington, MN
- R. K. Genung, Oak Ridge National Laboratory, Oak Ridge, TN
- J. G. Kay, Drexel University, Philadelphia, PA
- G. R. St. Pierre, Ohio State University, Columbus, OH
- J. Stringer, Electric Power Research Institute, Palo Alto, CA
- J. B. Wagner, Arizona State University, Tempe, AZ

T. Ahn, U. S. Nuclear Regulatory Commission, Washington, DC
D. H. Alexander, USDOE, Civilian Radioactive Waste Management, Washington, DC
J. Allison, USDOE, Office of Waste Management, Germantown, MD
S. Bates, Idaho Falls, ID
H. Benton, B&W Fuel Company, Las Vegas, NV
A. Berusch, USDOE, Office of Civilian Radioactive Waste Management, Washington, DC
N. E. Bibler, Westinghouse Savannah River Company, Aiken, SC
J. M. Boak, USDOE, Yucca Mountain Site, Las Vegas, NV
K. Boomer, Westinghouse Hanford Company, Richland, WA
W. Bourcier, Lawrence Livermore National Laboratory, Livermore, CA
E. T. Bramlitt, Defense Nuclear Agency, Kirtland Air Force Base, Kirtland, NM
A. Brandstetter, Science Applications, International Corporation, Las Vegas, NV
N. R. Brown, USDOE, Richland Operations Office, Richland, WA
J. Bucher, Lawrence Berkeley Laboratory, Berkeley, CA
J. Canepa, Los Alamos National Laboratory, Los Alamos, NM
K. A. Chacey, USDOE, Office of Environmental Management, Germantown, MD
D. Chestnut, Lawrence Livermore National Laboratory, Livermore, CA
G. R. Choppin, Florida State University, Tallahassee, FL
S. Clark, University of Georgia, Savannah River Ecology Laboratory, Aiken, SC
P. Cloke, Science Applications International Corp., Las Vegas, NV
M. O. Cloninger, Mac Technical Services, Inc., Richland, WA

D. Codell, U. S. Nuclear Regulatory Commission, Washington, DC
G. Colten-Bradley, U. S. Nuclear Regulatory Commission, Rockville, MD
S. Coplan, U. S. Nuclear Regulatory Commission, Washington, DC
S. P. Cowan, USDOE, Office of Waste Management, Germantown, MD
J. Davidson, U. S. Environmental Protection Agency, Washington, DC
J. Docka, Roy F. Weston, Inc., Washington, DC
R. Dresser, Roy F. Weston, Inc., Washington, DC
R. S. Dyer, Yucca Mountain Project Office, Las Vegas, NV
R. E. Erickson, USDOE, Office of Environmental Management, Germantown, MD
E. Essington, Los Alamos National Laboratory, Los Alamos, NM
F. M. Estes, Idaho State University, Pocatello, ID
R. C. Ewing, Department of Geology, University of New Mexico, Albuquerque, NM
D. Farr, Los Alamos National Laboratory, Los Alamos, NM
R. Fish, B&W Fuel Company, Las Vegas, NV
J. Gauthier, Sandia National Laboratories, Albuquerque, NM
F. Gelbard, Sandia National Laboratories, Albuquerque, NM
C. P. Gertz, USDOE, Yucca Mountain Project Office, Las Vegas, NV
S. E. Gomberg, USDOE, Office of Civilian Radioactive Waste Management, Washington, DC
W. Gray, Pacific Northwest Laboratories, Richland, WA
P. W. Hart, USDOE, Office of Technology Development, Germantown, MD
J. Hennessey, USDOE, Office of Waste Management, Germantown, MD
J. Herzog, Lockheed Idaho Technology Company, Idaho Falls, ID
D. Hobart, LANL, TTSO Group, Germantown, MD
J. Hunt, University of California, Berkeley, Berkeley, CA
D. Hutchins, Martin Marietta Systems, Inc., Oak Ridge, TN
C. Interrante, U.S. Nuclear Regulatory Commission, Washington, DC
C. Jantzen, Westinghouse Savannah River Company, Aiken, SC
L. J. Jardine, Lawrence Livermore National Laboratory, Livermore, CA
P. Kearl, Oak Ridge National Laboratory, Grand Junction, CO
J. Keith, Daniel B. Stephens & Associates, Albuquerque, NM
J. Kerrisk, Los Alamos National Laboratory, Los Alamos, NM
W. S. Ketola, USDOE, West Valley Project Office, West Valley, NY
D. A. Knecht, Lockheed Idaho Technology Company, Idaho Falls, ID
D. Kubosumi, Lockheed Idaho Technology Company, Idaho Falls, ID
W. L. Kuhn, Pacific Northwest Laboratories, Richland, WA
W. Lee, Environmental Evaluation Group, Albuquerque, NM
W. W. Lee, University of California, Berkeley, CA
J. C. Lehr, USDOE, Office of Environmental Restoration, Germantown, MD
H. Leider, Lawrence Livermore National Laboratory, Livermore, CA
R. A. Lemons, Los Alamos National Laboratory, Los Alamos, NM
S. Levy, Los Alamos National Laboratory, Los Alamos, NM
D. Livingston, USDOE, Yucca Mountain Site, Las Vegas, NV
J. J. Lorenz, USDOE, Yucca Mountain Site, Las Vegas, NV
R. Luce, Nuclear Waste Technical Review Board, Arlington, VA
W. Lutze, University of New Mexico, Albuquerque, NM
H. Manaktala, Southwest Research Institute, San Antonio, TX

S. Martin, Lawrence Livermore National Laboratory, Livermore, CA
J. M. Matuszek, JMM Consulting, Del Mar, NY
J. McCarthy, Oak Ridge National Laboratory, Oak Ridge, TN
L. McDowell-Boyer, Oak Ridge National Laboratory, Grand Junction, CO
T. W. McIntosh, USDOE, Office of Waste Management, Germantown, MD
J. Meldrum, University of Nevada - Las Vegas, Las Vegas, NV
A. Mitchell, Los Alamos National Laboratory, Los Alamos, NM
R. Morissette, Science Applications International Corp., Las Vegas, NV
D. Morris, Los Alamos National Laboratory, Los Alamos, NM
P. K. Nair, Southwest Research Institute, San Antonio, TX
S. Nelson, Las Vegas, NV
B. Newman, Los Alamos National Laboratory, Los Alamos, NM
C. Novak, Sandia National Laboratories, Albuquerque, NM
E. Nuttall, University of New Mexico, Albuquerque, NM
W. O'Connell, Lawrence Livermore National Laboratory, Livermore, CA
T. O'Holleran, Lockheed Idaho Technology Company, Idaho Falls, ID
G. C. S. Ordaz, USDOE, Office of Technology Development, Germantown, MD
C. Palmer, Lawrence Livermore National Laboratory, Livermore, CA
R. Palmer, West Valley Nuclear Services, West Valley, NY
H. Papenguth, Sandia National Laboratories, Albuquerque, NM
U-Sun Park, Science Applications International Corp., Las Vegas, NV
W. D. Pearson, Westinghouse Savannah River Company, Aiken, SC
C. Peterson, U. S. Nuclear Regulatory Commission, Washington, DC
T. H. Pigford, University of California, Berkeley, CA
M. J. Plodinec, Westinghouse Savannah River Company, Aiken, SC
W. Polzer, Los Alamos National Laboratory, Los Alamos, NM
W. G. Ramsey, Westinghouse Savannah River Company, Aiken, SC
P. Reimus, Los Alamos National Laboratory, Los Alamos, NM
B. Robinson, Los Alamos National Laboratory, Los Alamos, NM
P. Rogers, Los Alamos National Laboratory, Los Alamos, NM
R. Rundberg, Los Alamos National Laboratory, Los Alamos, NM
C. G. Russomanno, USDOE, Civilian Radioactive Waste Management, Washington, DC
J. Ryan, University of Colorado, Boulder, CO
R. Schulze, Los Alamos National Laboratory, Los Alamos, NM
W. C. Schutte, USDOE, Office of Technology Development, Germantown, MD
M. Siegel, Sandia National Laboratories, Albuquerque, NM
M. Silva, Environmental Evaluation Group, Albuquerque, NM
R. Silva, Lawrence Livermore National Laboratory, Livermore, CA
A. Simmons, USDOE, Las Vegas, NV
E. Springer, Los Alamos National Laboratory, Los Alamos, NM
J. Sproull, Westinghouse Savannah River Company, Aiken, SC
D. Stahl, M&O/B&W Fuel Company, Las Vegas, NV
B. Staples, Lockheed Idaho Technology Company, Idaho Falls, ID
W. Steinkampf, U.S. Geological Survey, Lakewood, CO
L. Stetzenbach, University of Nevada - Las Vegas, Las Vegas, NV
R. B. Stout, Lawrence Livermore National Laboratory, Livermore, CA

D. Strachan, Battelle Pacific Northwest Laboratories, Richland, WA
M. Tomozawa, Rensselaer Polytechnic Institute, Troy, NY
V. Trice, USDOE, Office of Waste Management, Germantown, MD
D. Turner, Southwest Research Institute, San Antonio, TX
B. Viani, Lawrence Livermore National Laboratory, Livermore, CA
K. Vinjamuri, Lockheed Idaho Technology Company, Idaho Falls, ID
J. Wan, New Mexico Tech, Socorro, NM
L. Wang, University of New Mexico, Albuquerque, NM
M. Whitbeck, Desert Research Institute, University of Nevada, Reno, NV
G. Willow, Lockheed Idaho Technology Company, Idaho Falls, ID
C. N. Wilson, Westinghouse Hanford Company, Richland, WA
J. Wilson, New Mexico Tech, Socorro, NM
M. Wilson, Sandia National Laboratories, Albuquerque, NM
J. H. Wolfram, Biotechnology-INTEL, Montana State University, Bozeman, MT
K. Wolfsberg, Los Alamos National Laboratory, Los Alamos, NM
A. Wollerman, Science Applications International Corp., Germantown, MD
A. Yang, U.S. Geological Survey, Denver, CO
M. P. Gardiner, Harwell Laboratory, Didcot, Oxon, UNITED KINGDOM
B. Grambow, Kernforschungszentrum Karlsruhe, GmbH, GERMANY
J. Kim, Kernforschungszentrum Karlsruhe, GERMANY
H. Nitsche, Forschungszentrum Rossendorf e.V., GERMANY
T. Payne, Australian Nuclear Science and Technology Organization, AUSTRALIA
P. Van Iseghem, Boeretang, BELGIUM
E. Vernaz, Centre d'Etudes Nucleares de la Valle du Rhone, Marcoule, FRANCE
P. Vilks, Atomic Energy of Canada, Whiteshell Laboratories, Pinawa, Manitoba, CANADA
L. Werme, Svensk Karnbranslehantering AB, Stockholm, SWEDEN